Combination image flow cytometry for single-cell analysis reveals novel methods for isolating subsets of megakaryocyte progenitor populations

Lucas M. Bush, James E. Marvin and Tara L. Deans

Megakaryocytes (MKs) are rare cells that develop in the bone marrow and give rise to platelets. A major challenge in studying megakaryocyte development, and the diseases that arise from these cells, is the identification and classification of MK progenitor cells that are produced during hematopoiesis. Here, we utilize combination image flow cytometry to definitively identify rare progenitor cell populations originating from a heterogeneous sample of bone marrow cells using minimal antibody panels that can be used to isolate these rare cell populations.

Biological imaging in the form of microscopy has existed for centuries, with the most widely adopted application emerging in the form of fluorescence imaging. Fluorescent images capture biological snapshots of cellular processes that provide insight into function, yet imaging technologies are historically nonspecific and rely on qualitative, macroscopic localization events to establish a change in phenotype[1]. The advent of flow cytometry in the mid-20th century was followed by an explosion of quantitative, application driven techniques: retrospective analysis of DNA content in human tumors[2], immunophenotyping of hematological malignancies[3], seventeen-color analysis of the immune system[4] and more[5-7]. However, the lack of imaging modalities associated with conventional flow cytometry has led to poor resolution in subcellular co-localization assays. Image flow cytometry combines the detailed spatial resolution of fluorescence imaging with the quantitative power of flow cytometry to overcome these limitations, enabling the categorical identification of rare cellular events within heterogeneous cell populations.

The principle goal of this study is to verify the phenotypic identity of rare cell populations initially characterized with flow cytometry by analyzing associated image files simultaneously. Applying image processing techniques to select cells with fluorescence restricted to the edge validates that antibody staining represents true surface marker expression and eliminates possible misinterpretation of results due to autofluorescence or nonspecific staining of debris. Furthermore, analysis of cellular features in associated brightfield images reveals a correlation between surface marker expression, cell size and circularity, and cellular identity. Using combination image flow cytometry, we definitively identified hematopoietic stem cells (HSCs), elusive subsets of megakaryocyte (MKs) progenitors, and mature MKs with minimal antibody panels, ultimately simplifying complex multicolor staining protocols typically used to identify rare cell types in a heterogeneous population.

HSCs are capable of producing all cells of the blood lineage throughout the lifetime of an individual by balancing self-renewal with differentiation[8]. In the mouse, HSCs are broadly defined by the Lin-Sca1^{+}cKit^{+} (LSK) immunophenotype[9,10], where HSCs capable of long-term bone marrow (BM) reconstitution (LT-HSCs) are defined by expression of Thy1.1 and CD150, but lack expression of CD34 and FLT3. HSCs capable of short-term hematopoietic reconstitution (ST-HSCs) are defined by expression of CD34 and FLT3, but have lost expression of CD150. In the classic model of hematopoietic differentiation, ST-HSCs progress towards a multipotent progenitor (MPP) that has no self-renewal capacity, actively differentiates into all cells of the blood lineage, and is further defined by loss of Thy1.1 expression[9-11]. Recent studies suggest an alternative to the classic model of hematopoiesis; HSCs may undergo myeloid bypass to directly yield lineage-restricted myeloid progenitors (LRMPs) capable of clonal expansion and terminal differentiation into mature cell types[12,13]. Interestingly, three distinct subsets of LRMPs capable of prolonged MK repopulation exist: the common myeloid repopulating progenitor (CMRP), the megakaryocyte-erythroid repopulation progenitor (MERP), and the megakaryocyte repopulating progenitor (MKRP)[12]. To study these unique progenitor subpopulations, we capitalized on thrombopoietin (TPO)/c-Mpl signaling within the hematopoietic compartment. TPO/c-Mpl signaling is essential for self-renewal, survival, proliferation and differentiation into mature MKs[8,12,14-18]. Commitment down the MK lineage is characterized by an increase in cell size, endoreplication to increase DNA content, upregulation of MK-specific surface markers, and cytoplasmic remodeling to prepare for platelet production[16,17]. Although fundamental to the health of the animal, HSCs and MKs are extremely rare cell types that constitute approximately 0.5% and 0.01% of the mouse BM, respectively, presenting complications for large-scale studies[19,20].

Here, we quantified the effect of TPO on HSCs, MK progenitors, and mature MKs stained with two different antibody panels (Supplementary Table 1) using the ImageStream®X Mark II Imaging Flow Cytometer. Fresh BM cells isolated from mouse femurs were either directly analyzed, or cultured for 3 days with 50ng/mL recombinant murine TPO, then analyzed on the imaging flow cytometer. At both time points, cells were stained with LSK and MK antibody panels (Supplementary Table 1). Using only LSK antibodies, we identified canonical HSC populations and an HSC-derived MKRP population capable of proliferating in response to TPO/c-Mpl signaling (Fig. 1). Additionally, two antibodies or less were used to quantify enrichment of distinct MK progenitor subsets and mature MKs following TPO exposure (Fig. 2).

Initial quantitative flow cytometry plots were generated to stratify major subpopulations (Supplementary Fig. 1), then each subpopulation was further characterized by inspecting associated image files of individual flow cytometric events. In the absence of TPO, BM cells stained with LSK antibodies display four distinct cell populations (Fig. 1A). The percentage of Lin^{-} cells decreased while total Sca-1 and c-

Kit expression increased in response to TPO (Fig. 1B), indicating differentiation of HSCs into Lin^+ cells and self-renewal of LT- and ST-HSC subpopulations (Supplementary Fig. 2). Moreover, the subpopulations of Lin^- cells shifted, changing the landscape of Sca-1 vs. c-Kit intensity plots (Fig. 1, Supplementary Fig. 3). Near complete loss of $Lin^-Sca1^-cKit^-$ (R1) cells indicates that R1 cells no longer retain the capacity for self-renewal, but are primed for differentiation into cells expressing lineage markers. Lin-$Sca1^+$c-$Kit^{low/-}$ (R2) cells are enriched after culture with TPO, suggesting an LRMP that has symmetrically divided to self-renew. Lin-Sca-1^+c-Kit^+ (R3) cells are the classic rare LSK population that proliferates and retains high levels of Sca-1/c-Kit expression in response to TPO/c-Mpl signaling. Lin-Sca-1^{low}/c-Kit^+ (R4) cells also self-renew in response to TPO, suggesting a second, separate LRMP within the Lin^- BM compartment[10,12,13]. Image analysis of individual flow cytometric events without exposure to TPO (Fig. 1C, Supplementary Fig. 4A-D) and in the presence of TPO (Fig. 1D, Supplementary Fig. 4E-H) reveals more about the phenotype of each subpopulation. To investigate the effect of TPO on shape and size, brightfield images were analyzed. Plotting circularity vs. area of each subpopulation revealed that R4 cells were the largest, most circular cell type of the lineage negative cells, a property that was exaggerated after culture with TPO (Supplementary Fig. 5). Because MK maturation is marked by an increase in cell size, these cells were considered MERP/MKRP cells that can still respond to stem cell factor (SCF) signaling but have not yet initiated expression of lineage markers[10,17]. To our knowledge, this is the first report to use only LSK antibodies to quantify early enrichment of MK progenitors after stimulation with TPO. This serves as a novel method for proliferating MK progenitors that may provide insight to the early stages of MK commitment and development.

To identify mature MKs, cells were stained with a panel of antibodies and DNA dyes before and after exposure to TPO (Supplementary Fig. 6). The MK stain contained antibodies against the blood lineage surface markers CD45, CD41 and CD42d, and a Hoechst 33342 DNA dye. In response to TPO, overall expression of CD45, CD41, and CD42d increased (Supplementary Fig. 7A-C), and DNA ploidy of the main population of cells increased in intensity and uniformity (Supplementary Fig. 7D). Flow cytometry plots of CD45 vs. CD41 intensity were generated for both time points and seven subpopulations (R1-R7, respectively) with distinct expression levels were identified (Fig. 2). The percentage of cells in subpopulations R1 and R2 decreased after culture with TPO, while the percentage of cells in R3-R7 increased, respectively (Fig. 2, Supplementary Fig. 8).

R1 cells are $CD45^-CD41^-CD42d^-$, contain DNA, do not proliferate in response to TPO, and are highly prevalent in unstimulated BM, representative of a subpopulation of cells that cannot self-renew and is primed for differentiation. R2 cells express only CD45 and do not proliferate in response to TPO, indicating an MPP that dies or differentiates but cannot self-renew. R3 cells proliferate massively in

response to TPO and upregulate CD45, CD41, and CD42d expression. This demonstrates an initial CMRP phenotype that can self-renew or directly gives rise to MKRPs after culture with TPO. R4 cells emerge as a true subpopulation after TPO stimulation and are marked by low surface marker expression and DNA content, indicating an MERPs that can self-renew in response to TPO but have low MK production potential. R5 cells are $CD45^{-}CD41^{low}CD42d^{-}$ and lack nuclei, which is typical of maturing reticulocytes. R6 cells are $CD45^{-/low}CD41^{+}CD42d^{+}$ cells with low DNA content, exemplary of an LT-HSC-derived MKRP that can self-renew but has not yet undergone endoreplication to increase ploidy [9,10,12]. R7 cells are enriched after TPO stimulation, express the highest levels of all surface markers and are highly ploidy, indicative of mature MKs produced through asymmetric cell division of CMRPs, MERPs, or MKRPs[12], respectively (Supplementary Fig. 9).

Inspection of image files associated with individual events in each subpopulation confirms the phenotypic identities determined by flow cytometry. MKs are large cells that adhere to the vascular endothelial surface and extend cytoplasmic protrusions into sinusoidal blood vessels to produce platelets[17]. Analysis of R7 image files confirms R7 cells as a true mature MKs (Fig. 2). R7 cells were the subpopulation with the lowest circularity score and largest area both before and after TPO exposure (Supplementary Fig. 10), characteristics expected of mature MKs. Additionally, the associated fluorescent images (Supplementary Fig. 11) revealed bona fide co-expression of surface markers and multilobed, polyploid nuclei within the confines of the cell membrane. Because the R7 subpopulation has the highest CD45, CD41, and CD42d expression with the most DNA, it is feasible to use single-color stains with any of these markers in a typical flow cytometry experiment to isolate MKs for downstream functional analysis (Supplementary Fig. 12).

The methodology presented here has enabled the discovery of a previously unidentified MK progenitor cell population using minimal antibody panels. This discovery can significantly accelerate the identification of MK progenitor cells for improving our understanding of hematopoiesis and the formation of MK cells. Furthermore, these methods may also provide a better understanding of the molecular mechanisms underlying normal MK and platelet production that can improve targeted therapies for diseases that arise from skewed cell fate decisions, in addition to informing alternative approaches to produce megakaryocytes and platelets in vitro.

Methods

Bone marrow dissection and cell culture

Mice were maintained at the University of Utah under IACUC approved guidelines. The use of animal and/or animal-derived materials in this study was carrier out in accordance with relevant guidelines and regulations.

Mice were euthanatized by CO2 asphyxiation, followed by cervical dislocation. Femurs were dissected from the mouse, excess tissue was removed, and the epiphyses were snipped off. Bone marrow was then flushed with IMDM (ThermoFisher Scientific, #12440053) + 10% FBS (Gibco, #16000044) and 1X Penicillin-Streptomycin (ThermoFisher Scientific, #15140122) using a 26.5-guage needle and collected in a 35mm dish. Red blood cells were lysed using ACK Lysis Buffer (ThermoFisher Scientific, # A1049201) for 5 min at room temperature (RT), and then the solution was centrifuged at 300xg for 5 min. The cells were washed 3x with HBSS (Gibco, #14025092) then counted using a hemocytometer. If cells were cultured before analysis, $1x10^7$ cells were incubated in IMDM + 10% FBS supplemented with 50 ng/mL of recombinant murine TPO (PeproTech, #315-14) in a T75 flask at 37 °C in 5% CO_2 for 72 h.

Staining reagents

The following antibodies and DNA dyes were used: PE-Cy™7 Rat anti-Mouse CD117 (BD Pharmingen, #561681; 1:133 dilution), PE Rat Anti-Mouse Ly-6A/E (BD Pharmingen, #562059; 1:100 dilution), APC Mouse Lineage Antibody Cocktail (BD Pharmingen, #558074; 1:50 dilution), CD45 Monoclonal Antibody (ThermoFisher, #25-0451-81), PE-Cyanine7 (eBioscience™, #25-0451-81; 1:133 dilution), PE Rat Anti-Mouse CD41 (BD Pharmingen, #561850; 1:100 dilution), CD42d Monoclonal Antibody (1C2), APC (eBioscience™, #17-0421-80; 1:50 dilution), Hoechst 33342 Solution (BD Pharmingen; #561908, 1:1000 dilution), DAPI (ThermoFisher Scientific, #62247; 1:1000 dilution), 7-AAD Viability Staining Solution (eBioscience™, #00-6993-50; 1:100 dilution), and SYTOX™ Green Dead Cell Stain (ThermoFisher Scientific, #S34860; 1:1000 dilution).

Preparation for image flow cytometry

After isolation from the bone marrow, or culture with TPO for 72 h, cells were washed 2x with PBS. For the LSK stain, cells were resuspended in PBS + 3% BSA (ThermoFisher Scientific, #BP1600-100) with the addition of PE-Cy™7 Rat anti-Mouse CD117, PE Rat Anti-Mouse Ly-6A/E, and APC Mouse Lineage Antibody Cocktail, and incubated on ice protected from light for 30 min. Cells were washed 2x with PBS and resuspended at a final concentration of $2x10^7$ cells/mL in PBS. DAPI was added at least 5 min before running the sample on the image flow cytometer.

For the MK stain, cells were resuspended in prewarmed IMDM + 10% FBS containing the Hoechst 33342 solution, then incubated at 37 °C for 45 min. Cells were washed with PBS then resuspended in PBS + 3% BSA with the addition of PE-Cyanine7 CD45 Monoclonal Antibody, PE Rat Anti-Mouse CD41, and APC CD42d Monoclonal Antibody and incubated on ice, protected from light for 30 min. Cells were washed 2x with PBS then resuspended at a final concentration of $2x10^7$ cells/mL in PBS. 7-AAD was added at least 5 min before running the sample on the image flow cytometer.

Image flow cytometry data acquisition and analysis

Data from image flow cytometry experiments was acquired by gating for events that were in focus, did not contain calibration focus beads, and excluded viability dyes (Supplemental Fig. 1,6). All experiments used the ImageStream®X Mark II Imaging Flow Cytometer and all analysis was performed using the IDEAS® Software.

For the LSK stain, mean fluorescence intensity (MFI) values were calculated by plotting live cell intensity of Lineage Cocktail, Sca1, and cKit staining, then taking the average value of the plot (Supplemental Fig. 2). Further analysis of live cells by subgating for Lineage Negative cells resulted in Sca1 vs. cKit intensity plots (Supplemental Fig. 1, Fig. 2). The shifts in the four subpopulations – R1, R2, R3, and R4, respectively – were quantified by calculating the percentage of cells in each subpopulation before and after exposure to TPO (Supplemental Fig. 3). Additional image files for each of the four subpopulations were chosen based on surface marker expression and image quality (Supplemental Fig. 4). The IDEAS® Software was used to calculate the circularity of brightfield images. Plots of Brightfield Circularity vs. Area were generated before and after TPO exposure for each of the four subpopulations and overlaid (Supplemental Fig. 5a,b). Mean Brightfield Circularity vs. Area scores were generated by taking the average circularity and area of each of the four subpopulations (Supplemental Fig. 5c).

For the MK stain, MFI values were calculated by plotting live cell intensity of CD45, CD41, CD42d and Hoechst 33342 staining, then taking the average value of the plot (Supplemental Fig. 7). Direct plotting of live cell CD45 vs. CD41 intensity resulted in identification of the seven subpopulations – R1, R2, R3, R4, R5, R6, and R7, respectively. Shifts in these subpopulations were quantified by calculating the percentage of cells in each subpopulation before and after exposure to TPO (Supplemental Fig. 8). To characterize the cells in individual subpopulations, intensity of CD45, CD41, CD42d and Hoechst 33342 for each subpopulation were overlaid and averages were taken to produce MFI graphs (Supplemental Fig. 9). The IDEAS® Software was used to calculate the circularity of brightfield images. Plots of brightfield circularity vs. area were generated before and after TPO exposure for each of the four subpopulations and overlaid (Supplemental Fig. 10a,b). Mean brightfield circularity vs. area scores were generated by taking the average circularity and area of each of the seven subpopulations (Supplemental Fig. 10c). Additional image files for each of the seven subpopulations were chosen based on surface marker expression and image quality (Supplemental Fig. 11).

Fluorescence activated cell sorting (FACS) single-stained megakaryocytes

Following isolation from bone marrow or culture with TPO, cells were washed 2x with PBS. The Hoechst 33342 group was resuspended in prewarmed IMDM + 10% FBS containing the Hoechst 33342 solution, then incubated at 37 °C for 45 min. These cells were washed 1x with PBS, then the samples were resuspended in PBS + 3% BSA with the addition of PE-Cyanine7 CD45 Monoclonal Antibody for the CD45 stain, PE Rat Anti-Mouse CD41 for the CD41 stain, and APC CD42d Monoclonal Antibody for the CD42d stain, respectively. Cells were incubated on ice, protected from light for 30 min, then washed 2x with PBS and resuspended in a final volume of 200 µL. Cells were sorted into IMDM + 10% FBS using the BD FACSAria III, then plated into a 24-well cell culture dish. Images were taken using the EVOS FL Auto 2 Cell Imaging System. All FACS data analysis was performed using FlowJo®.

Acknowledgements

We gratefully acknowledge the funding from the University of Utah startup funds, the National Science Foundation CAREER Program (CBET-1554017), the Office of Naval Research Young Investigator Program (N00014-16-1-3012), the National Institute of Health Trailblazer Award (1R21EB025413-01), and the NIH Ruth L. Kirschstein National Research Service Award NIH from the National Institute of Diabetes and Digestive and Kidney Diseases (5T32DK007115-42). This work was also supported by the University of Utah Flow Cytometry Facility, the University of Utah Fluorescence Microscopy Core Facility (1S10RR024761-01), the National Cancer Institute (5P30CA042014-24), and the National Center for Research of the National Institutes of Health (1S10RR026802-01). We thank Dr. Charles Voyton, Dr. Ken A. Christensen and Dr. Josh Andersen of the BYU Department of Chemistry & Cancer Discovery for use of the ImageStream®X Mark II Imaging Flow Cytometer. For technical expertise with imaging flow cytometry analyses, we thank Dr. Amal El-Mabhouh, Ph.D. – MilliporeSigma, USA.

Author contributions

LMB conducted all of the experiments and analyzed the data. TLD and JEM helped design experiments and analyze data. LMB and TLD wrote the manuscript.

Competing interests

The authors declare no competing financial interest.

References:

1 Massoud, T. F. & Gambhir, S. S. Molecular imaging in living subjects: seeing fundamental biological processes in a new light. *Genes & development* **17**, 545-580, doi:10.1101/gad.1047403 (2003).

2 Hedley, D. W., Friedlander, M. L., Taylor, I. W., Rugg, C. A. & Musgrove, E. A. Method for analysis of cellular DNA content of paraffin-embedded pathological material using flow cytometry. *J Histochem Cytochem* **31**, 1333-1335, doi:10.1177/31.11.6619538 (1983).

3 Brown, M. & Wittwer, C. Flow cytometry: principles and clinical applications in hematology. *Clin Chem* **46**, 1221-1229 (2000).

4 Perfetto, S. P., Chattopadhyay, P. K. & Roederer, M. Seventeen-colour flow cytometry: unravelling the immune system. *Nature reviews. Immunology* **4**, 648-655, doi:10.1038/nri1416 (2004).

5 Alvarez-Barrientos, A., Arroyo, J., Canton, R., Nombela, C. & Sanchez-Perez, M. Applications of flow cytometry to clinical microbiology. *Clin Microbiol Rev* **13**, 167-195 (2000).

6 Maino, V. C. & Picker, L. J. Identification of functional subsets by flow cytometry: intracellular detection of cytokine expression. *Cytometry* **34**, 207-215 (1998).

7 Vives-Rego, J., Lebaron, P. & Nebe-von Caron, G. Current and future applications of flow cytometry in aquatic microbiology. *FEMS Microbiol Rev* **24**, 429-448 (2000).

8 Seita, J. *et al.* Lnk negatively regulates self-renewal of hematopoietic stem cells by modifying thrombopoietin-mediated signal transduction. *Proceedings of the National Academy of Sciences of the United States of America* **104**, 2349-2354, doi:10.1073/pnas.0606238104 (2007).

9 Chang, Y., Bluteau, D., Debili, N. & Vainchenker, W. From hematopoietic stem cells to platelets. *Journal of thrombosis and haemostasis : JTH* **5 Suppl 1**, 318-327, doi:10.1111/j.1538-7836.2007.02472.x (2007).

10 Seita, J. & Weissman, I. L. Hematopoietic stem cell: self-renewal versus differentiation. *Wiley Interdiscip Rev Syst Biol Med* **2**, 640-653, doi:10.1002/wsbm.86 (2010).

11 Reya, T., Morrison, S. J., Clarke, M. F. & Weissman, I. L. Stem cells, cancer, and cancer stem cells. *Nature* **414**, 105-111, doi:10.1038/35102167 (2001).

12 Yamamoto, R. *et al.* Clonal analysis unveils self-renewing lineage-restricted progenitors generated directly from hematopoietic stem cells. *Cell* **154**, 1112-1126, doi:10.1016/j.cell.2013.08.007 (2013).

13 Paul, F. *et al.* Transcriptional Heterogeneity and Lineage Commitment in Myeloid Progenitors. *Cell* **163**, 1663-1677, doi:10.1016/j.cell.2015.11.013 (2015).

14 Buza-Vidas, N. *et al.* Cytokines regulate postnatal hematopoietic stem cell expansion: opposing roles of thrombopoietin and LNK. *Genes & development* **20**, 2018-2023, doi:10.1101/gad.385606 (2006).

15 Kirito, K., Fox, N. & Kaushansky, K. Thrombopoietin stimulates Hoxb4 expression: an explanation for the favorable effects of TPO on hematopoietic stem cells. *Blood* **102**, 3172-3178, doi:10.1182/blood-2003-03-0944 (2003).

16 Kaushansky, K. *et al.* Promotion of megakaryocyte progenitor expansion and differentiation by the c-Mpl ligand thrombopoietin. *Nature* **369**, 568-571, doi:10.1038/369568a0 (1994).

17 Machlus, K. R. & Italiano, J. E., Jr. The incredible journey: From megakaryocyte development to platelet formation. *The Journal of cell biology* **201**, 785-796, doi:10.1083/jcb.201304054 (2013).

18 Yoshihara, H. *et al.* Thrombopoietin/MPL signaling regulates hematopoietic stem cell quiescence and interaction with the osteoblastic niche. *Cell Stem Cell* **1**, 685-697, doi:10.1016/j.stem.2007.10.020 (2007).

19 Nakeff, A. & Maat, B. Separation of megakaryocytes from mouse bone marrow by velocity sedimentation. *Blood* **43**, 591-595 (1974).

20 Wilson, A. & Trumpp, A. Bone-marrow haematopoietic-stem-cell niches. *Nature reviews. Immunology* **6**, 93-106, doi:10.1038/nri1779 (2006).

Figures

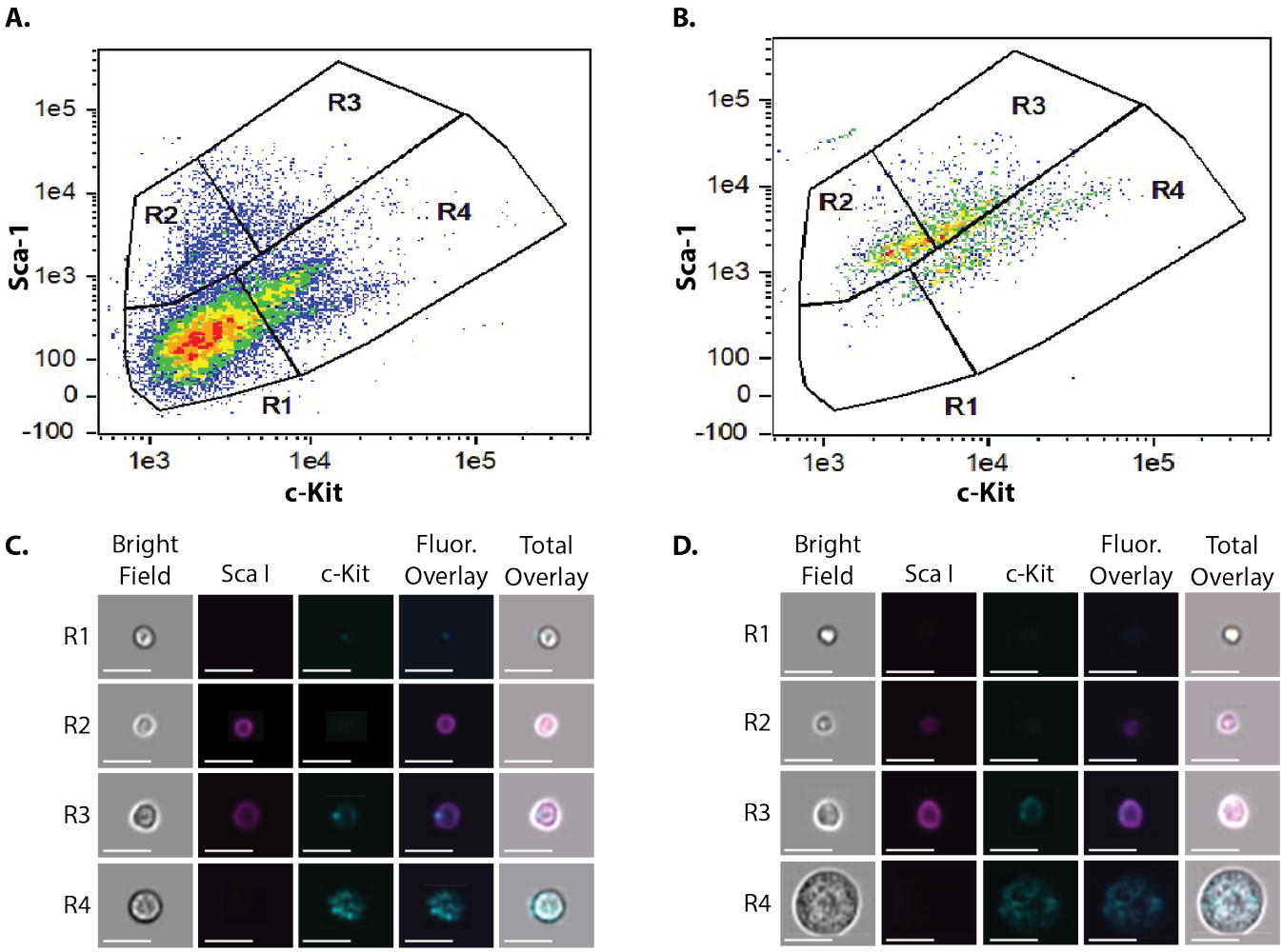

Figure 1: Image flow cytometry plots and representative images of cells stained with LSK antibodies. **A**. Flow cytometry plot of Sca1 intensity vs. cKit intensity for Lin$^-$ cells in the absence of TPO. **B**. Flow cytometry plot of Sca1 intensity vs. cKit intensity for Lin$^-$ cells in the presence of 50ng/ml of TPO for 3 days. **C**. Representative image panels of each subpopulation in the absence of TPO and **D**. in the presence of TPO. Scale bars, 20μm.

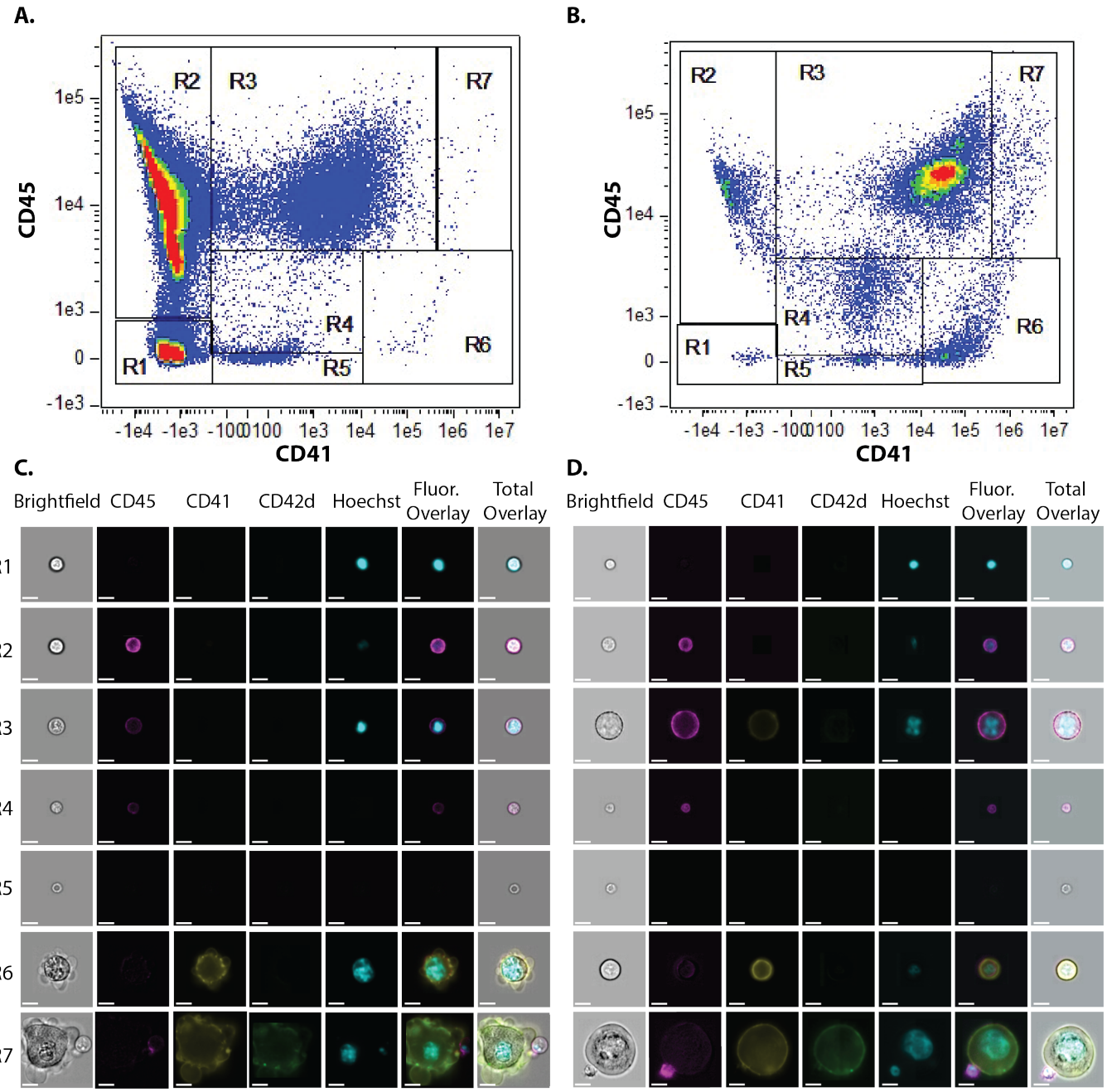

Figure 2: Image flow cytometry and representative images of cells stained with CD45 and CD41. **A**. Flow cytometry plot of CD45 intensity vs. CD41 intensity in the absence of TPO. **B**. Flow cytometry plot of CD45 intensity vs. CD41 intensity in the presence of TPO. **C**. Representative image panels of each subpopulation in the absence of TPO and **D**. in the presence of TPO for three days. Scale bars, 10μm.